Reprinted from THE JOURNAL OF THE ACOUSTICAL SOCIETY OF AMERICA, Vol. 40, No. 1, 179-186, July 1966

Axisymmetric Vibrations of Prolate Spheroidal Shells

F. DIMAGGIO AND R. RAND

Department of Civil Engineering and Engineering Mechanics, Columbia University, New York, New York

Nontorsional extensional axisymmetric modes and frequencies of elastic prolate spheroidal shells as a function of eccentricity are obtained by a numerical technique. The mode spectra have two distinct branches, analogous to those of spherical and cylindrical shells. Extensive results are presented for the lower branches.

LIST OF SYMBOLS

a	radial coordinate of shell middle surface, inverse of eccentricity of shell middle surface
c	frequency parameter defined by Eq. 4
d	interfocal distance; shown in Fig. 2
f_1, f_2, f_3	functions of η defined by Eq. 20
f_{1i}, f_{2i}, f_{3i}	values of f_1, f_2 and f_3 at pivotal point η_i
f_4, f_5, f_6	functions of η defined in Appendix A (Eqs. A4)
g	function of η defined in Appendix A (Eq. A3)
g_{1i}, g_{2i}, g_{3i}	linear combinations of f_{1i}, f_{2i}, and f_{3i} defined by Eq. 19
h	spacing of pivotal points and minimum shell thickness
i	index defining pivotal point; defined by Eq. 18
l	length of shell; see Fig. 2
n	mode number
p	index used in Eq. 9
r	ratio of major to minor axis of shell middle surface; see Eq. 33
t	time
u, w	tangential and radial displacements of points on shell middle surface; illustrated in Fig. 2
x	defined by Eq. 7
E	Young's modulus
N	number of equal intervals used in numerical integration; see Eq. 24
R	equatorial radius; see Fig. 2
S	function of η defined by Eq. 11
S_i	value of S at pivotal point η_i
U, W	mode shapes; see Eq. 1
U_i, W_i	values of U, W at pivotal points η_i
λ	frequency parameter defined by Eq. 31
μ	shear modulus
ν	Poisson's ratio
ω	natural frequency of shell; see Eq. 1
ρ	mass density of shell
ξ, η	radial and tangential ellipsoidal coordinates; illustrated in Fig. 1
ϕ_1, ϕ_2, ϕ_3	polynomials in x defined by Eqs. 2, 3, and 8
ψ_1, ψ_2	functions of η written out in Appendix A (Eqs. A2)
δ_{1i}, ψ_{2i}	values of ψ_1 and ψ_2 at pivotal points η_i
$\theta_1, \theta_2, \theta_3$	functions of η written out in Appendix A (Eqs. A1)
X	frequency parameter defined by Eq. 32

INTRODUCTION

IN two previous investigations,[1,2] the Rayleigh–Ritz method and perturbation from the spherical geometry were used to obtain modes and frequencies of free, nontorsional, axisymmetric, extensional vibrations of elastic prolate spheroidal shells of small eccentricity *in vacuo*. Numerical results were obtained for ratios of

[1] A. Silbiger and F. DiMaggio, "Extensional Axisymmetric Second Class Vibrations of a Prolate Spheroidal Shell," Columbia Univ. Tech. Rept. No. 3, contract Nonr 266(67) (Feb. 1961).
[2] N. Shiraishi and F. DiMaggio, "Perturbation Solution for the Axisymmetric Vibrations of Prolate Spheroidal Shells," J. Acoust. Soc. Am. 34,1725-1731 (1962).

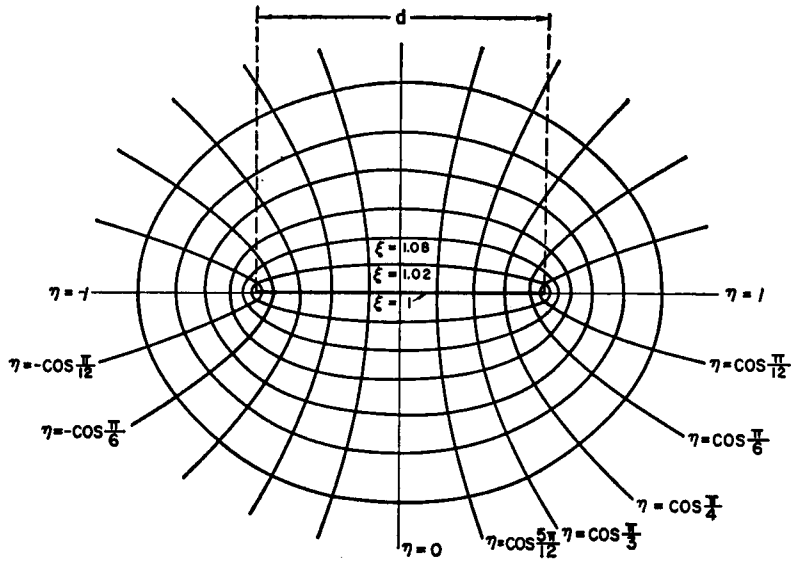

FIG. 1. Prolate spheroidal coordinate system.

major to minor axis, r, $\leq\sqrt{2}$. For larger eccentricities, these techniques proved impractical because of poor convergence.

In this paper, the radial displacement is first eliminated from the two governing differential equations of motion. The remaining equation on the tangential displacement has two regular singular points. By an appropriate change of dependent variable, a single second-order differential equation on an analytic function is obtained, whose numerical solution yields modes and frequencies for any eccentricity.

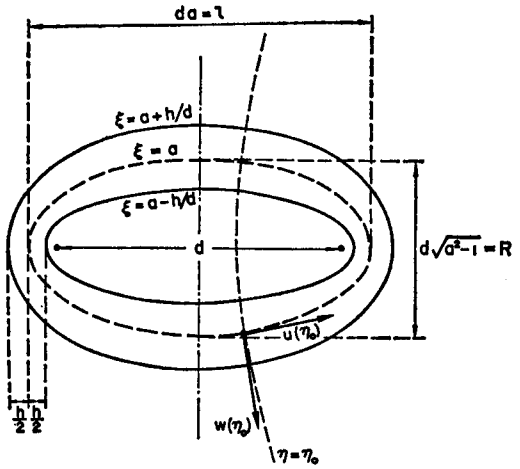

FIG. 2. Geometry of structure.

I. FORMULATION OF THE PROBLEM

Using Flammer's notation,[3] the prolate spheroidal coordinate system and geometry of the structure are shown in Figs. 1 and 2.

The shell is assumed to be bounded by confocal spheroids defined by $\xi=a\pm h/d$, where d is the interfocal distance, h is the minimum thickness, and $\xi=a$ (eccentricity is $1/a$), the middle surface. The displacements w and u, respectively perpendicular and tangent to the middle surface, are termed radial and tangential.

The equations satisfied by the tangential and radial modes $U(\eta)$ and $W(\eta)$, defined by

$$u(\eta,t)=U(\eta)e^{i\omega t},\quad w(\eta,t)=W(\eta)e^{i\omega t},\tag{1}$$

in which ω is the natural frequency, are[1,2]

$$-(1-\eta^2)^{\frac{1}{2}}\frac{d^2}{d\eta^2}[(1-\eta^2)^{\frac{1}{2}}U]-(1-\nu)U-(1-\eta^2)^{\frac{1}{2}}\frac{d}{d\eta}\left\{\left[\frac{\nu}{(a^2-1)^{\frac{1}{2}}}+\frac{(a^2-1)^{\frac{1}{2}}}{a^2-\eta^2}\right]aW\right\}$$
$$-\frac{(1-\nu)\eta(1-\eta^2)^{\frac{1}{2}}}{(a^2-1)^{\frac{1}{2}}(a^2-\eta^2)}aW=\frac{1-\nu}{2}c^2(a^2-\eta^2)U,\tag{2}$$

$$\left[\frac{\nu}{(a^2-1)^{\frac{1}{2}}}+\frac{(a^2-1)^{\frac{1}{2}}}{a^2-\eta^2}\right]\frac{d}{d\eta}[(1-\eta^2)^{\frac{1}{2}}aU]-\frac{(1-\nu)\eta(1-\eta^2)^{\frac{1}{2}}}{(a^2-1)^{\frac{1}{2}}(a^2-\eta^2)}aU+\left[\frac{1}{a^2-1}+\frac{2\nu}{a^2-\eta^2}+\frac{a^2-1}{(a^2-\eta^2)^2}\right]a^2W=\frac{1-\nu}{2}c^2(a^2-\eta^2)W,\tag{3}$$

[3] C. Flammer, *Spheroidal Wave Functions* (Stanford University Press, Stanford, Calif., 1957).

where ν is Poisson's ratio and

$$c^2=\rho\omega^2d^2/4\mu, \tag{4}$$

in which ρ is the mass density of the shell material and μ its shear modulus. The natural boundary conditions associated with Eqs. 2 and 3 are

$$U(\pm1)=0, \tag{5}$$

$$W(\pm1) \text{ IS BOUNDED.} \tag{6}$$

Letting

$$x=1-\eta^2, \tag{7}$$

solving Eq. 3 for W, and substituting into Eq. 2 yields

$$x^2\phi_1\frac{d^2U}{dx^2}+x\phi_2\frac{dU}{dx}+\phi_3U=0, \tag{8}$$

where ϕ_1, ϕ_2 and ϕ_3 are polynomials in x, each containing a constant term. If a solution of the form

$$U=x^m\sum_{p=0}^{\infty}a_px^p, \tag{9}$$

is substituted into Eq. 8, and the coefficient of the term containing the lowest power of x—namely, x^m—is set equal to zero, one obtains

$$m=\pm\tfrac{1}{2}. \tag{10}$$

To satisfy Eq. 5, choose $m=\frac{1}{2}$. Thus,

$$\begin{aligned}U&=(1-\eta^2)^{\frac{1}{2}}[a_0+a_1(1-\eta^2)+a_2(1-\eta^2)^2+\cdots]\\&=(1-\eta^2)^{-\frac{1}{2}}[a_0(1-\eta^2)\\&\qquad+a_1(1-\eta^2)^2+a_2(1-\eta^2)^3+\cdots]\\&=(1-\eta^2)^{-\frac{1}{2}}S(\eta),\end{aligned} \tag{11}$$

where S is an analytic function of η while $U(\eta)$ had regular singular points at $\eta=\pm1$.

Substituting Eq. 11 into Eqs. 8 and 3 yields

$$(1-\eta^2)\theta_1\frac{d^2S}{d\eta^2}+(1-\eta^2)\theta_2\frac{dS}{d\eta}+\theta_3S=0, \tag{12}$$

where θ_1, θ_2, and θ_3 are polynomials in η, written out explicitly in Appendix A, and

$$W=\psi_1\frac{dS}{d\eta}+\psi_2S, \tag{13}$$

where ψ_1 and ψ_2 are functions of η also written out in Appendix A.

From Eqs. 5 and 11, it is seen that S satisfied the boundary conditions

$$S(\pm1)=0. \tag{14}$$

For the symmetric modes, $U(\eta)=-U(-\eta)$. Thus, from Eq. 11,

$$S(\eta)=-S(-\eta). \tag{15}$$

Similarly, for the antisymmetric modes,

$$S(\eta)=S(-\eta). \tag{16}$$

By using one of the conditions of Eq. 14 and either Eq. 15 or 16 as appropriate, only one-half the shell need be considered in the analysis.

II. NUMERICAL TECHNIQUE FOR DETERMINATION OF MODES AND FREQUENCIES

If the derivatives in Eq. 12 are replaced by their central difference expansions with error of order h^2, where h is the spacing of the pivotal points, there results the recurrence equation

$$S_{i+1}=-(g_{1i})^{-1}(g_{2i}S_i+g_{3i}S_{i-1}), \tag{17}$$

in which

$$i=\eta_i/h; \tag{18}$$

$$\begin{aligned}g_{1i}&=(2/h)f_{1i}+f_{2i},\\g_{2i}&=-(4/h)f_{1i}+2hf_{3i},\\g_{3i}&=(2/h)f_{1i}-f_{2i};\end{aligned} \tag{19}$$

$$\begin{aligned}f_1&=\theta_1(1-\eta^2),\\f_2&=\theta_2(1-\eta^2),\\f_3&=\theta_3.\end{aligned} \tag{20}$$

The boundary conditions of Eqs. 14–16 become

$$S_N=0, \tag{21}$$

$$S_{-1}=-S_1, \quad \text{for symmetric modes} \tag{22}$$

$$S_{-1}=S_1, \quad \text{for antisymmetric modes} \tag{23}$$

where, from Eq. 18,

$$N=1/h. \tag{24}$$

Setting $i=0$ in Eq. 17 and substituting Eqs. 22 and 23 into it gives

$$S_0=[(g_{10}\pm g_{30})/-g_{20}]S_1, \tag{25}$$

where the $(-,+)$ sign refers to (symmetric, antisymmetric) modes. Since the amplitude of the mode is arbitrary, S_1 is selected so that $U_1=1$. From Eqs. 11 and 18

$$U_i=S_i(1-i^2h^2)^{-\frac{1}{2}}, \tag{26}$$

from which

$$S_1=1\cdot(1-h^2)^{\frac{1}{2}}. \tag{27}$$

Starting with the values of S_1 and S_0 from Eqs. 25 and 27 and assuming a value of the frequency param-

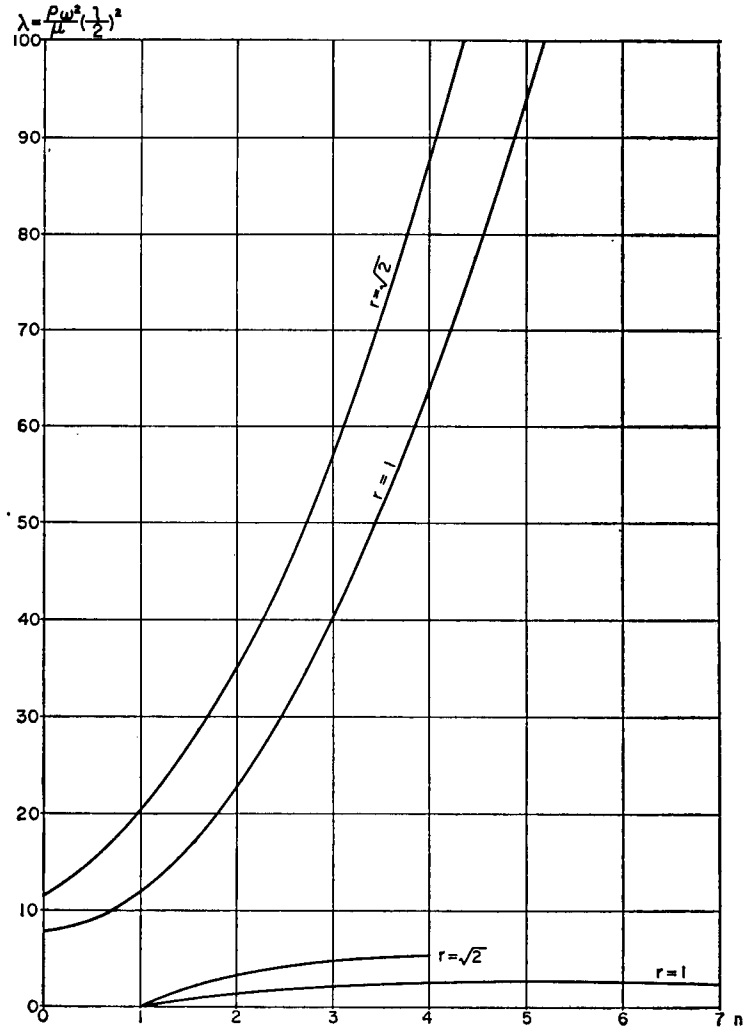

FIG. 3. Upper and lower branches of mode spectrum for a spherical shell ($r=1$) and a spheroidal shell with ratio $r=l/R$ of length to equatorial radius $=\sqrt{2}$, for $\nu=\frac{1}{3}$.

eter c^2 of Eq. 4, Eq. 17 may be used to obtain S_N by forward integration:

$$S_N=\frac{-1}{g_{1,N-1}}(g_{2,N-1}S_{N-1}+g_{3,N-1}S_{N-2}). \tag{28}$$

If the assumed value of c^2 corresponds to a natural frequency, the value of S_N obtained from Eq. 28 will satisfy Eq. 21. Thus by plotting S_N obtained from Eq. 28 as a function of the assumed value of c^2, the natural frequencies are obtained from the zeros of this plot.

The tangential mode shapes corresponding to each natural frequency and the values of S_i are obtained from Eq. 26. ($U_N=0$ is obtained from Eq. 5 since Eq. 26 is an indeterminate form for $i=N$.)

The radial mode shapes are now obtained from the central difference expansion of Eq. 13:

$$W_i=\psi_{1i}[(S_{i+1}-S_{i-1})/2h]+\psi_{2i}S_i. \tag{29}$$

Since U_{N+1} is not a physically meaningful point, W_N cannot be found from Eq. 29. It may be found by passing a parabola through W_{N-1}, W_{N-2}, and W_{N-3} and extrapolating a value of W_N from

$$W_N=3W_{N-1}-3W_{N-2}+W_{N-3}. \tag{30}$$

III. FREQUENCY PARAMETERS AND MODE SPECTRA

In order to exhibit the variation of frequency with eccentricity, it is desirable to introduce two particular frequency parameters derived from c^2 of Eq. 4. These are

$$\lambda=c^2a^2=\frac{\rho\omega^2}{\mu}\left(\frac{da}{2}\right)^2=\frac{\rho\omega^2}{\mu}\left(\frac{l}{2}\right)^2 \tag{31}$$

and

$$X=\lambda r^2=\frac{\rho\omega^2}{\mu}\left(\frac{d(a^2-1)^{\frac{1}{2}}}{2}\right)^2=\frac{\rho\omega^2}{\mu}\left(\frac{R}{2}\right)^2, \tag{32}$$

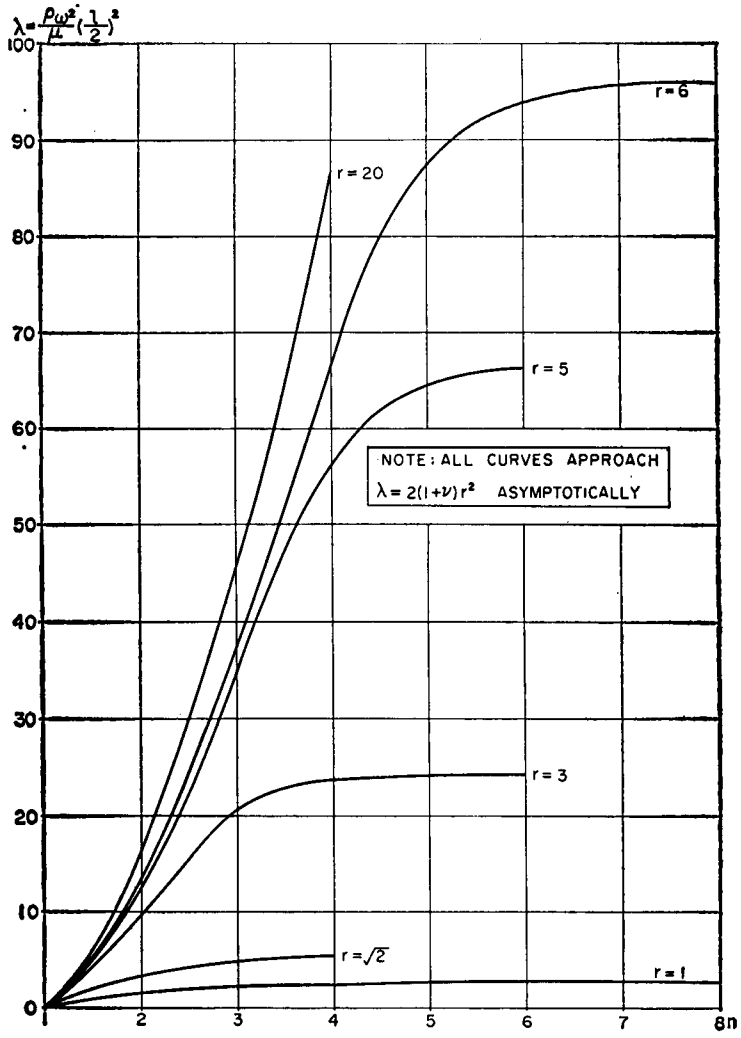

FIG. 4. Lower branch of mode spectrum for shells of constant length l and varying ratios $r=l/R$ of length to equatorial radius for $\nu=\frac{1}{3}$.

where

$$r=a/(a^2-1)^{\frac{1}{2}}=l/R \tag{33}$$

is the ratio of major to minor axis of the shell middle surface. Referring to Fig. 2, it is seen that λ is a measure of frequency for shells of constant length with varying eccentricities, while X is the appropriate frequency parameter when comparing shells of constant equatorial radius.

It is expected that, just as in the case of a cylindrical[4] and spherical[5] shells, the mode spectrum (plot of X or λ versus mode number n) for a given eccentricity will have an upper and a lower branch and that the lower branch will asymptotically approach a limit value lower than the lowest frequency of the upper branch.

As the mode number increases, the limit frequency for any eccentricity should approach the frequency of radial vibration of a thin circular ring of mean radius equal to the equatorial radius of the shell middle surface since this happens in both the cylindrical and spherical geometry. Therefore,

$$\lim_{n\to\infty}\omega^2=[2\mu(1+\nu)/\rho][2/d(a^2-1)^{\frac{1}{2}}], \tag{34}$$

in which ν is Poisson's ratio. In terms of the frequency parameters λ and X and the ratio of major to minor axis r of Eqs. 31–33, Eq. 34 becomes

$$\lim_{n\to\infty}\lambda=2(1+\nu)r^2, \tag{35}$$

$$\lim_{n\to\infty}X=2(1+\nu). \tag{36}$$

Equation 36 states that the limit value of the frequency parameter X is independent of shell eccentricity.

[4] M. C. Junger and F. J. Rosato, "The Propagation of Elastic Waves in Thin-Walled Cylindrical Shells," J. Acoust. Soc. Am. 26, 709–713 (1954).

[5] H. Lamb, "On the Vibration of a Spherical Shell," Proc. London Math. Soc. 14, 50–56 (1883).

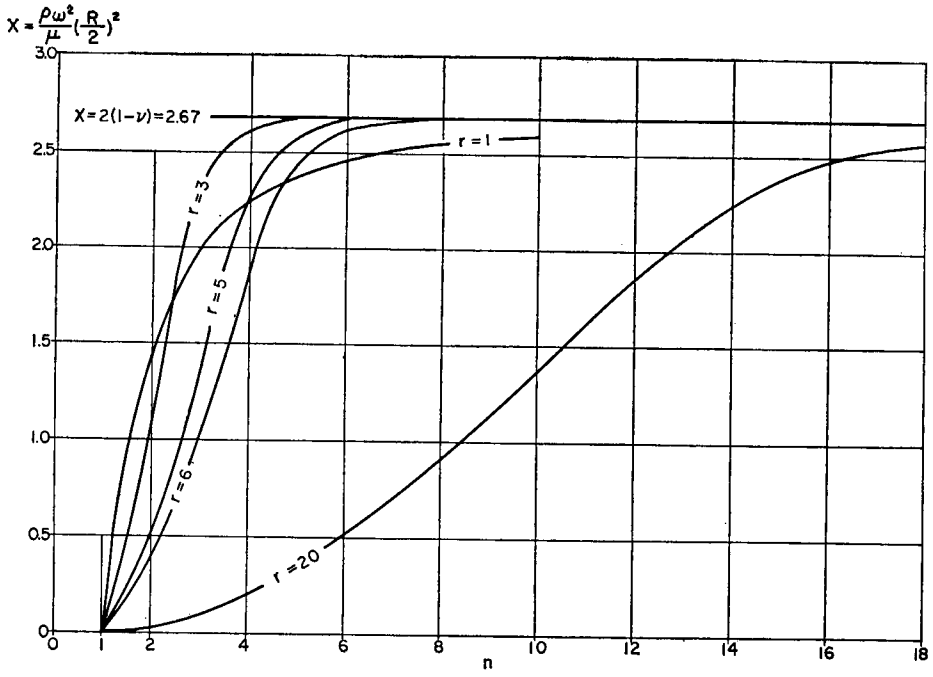

FIG. 5. Lower branch of mode spectrum for shells of constant equatorial radius R and varying ratios $r=l/R$ of length to equatorial radius for $\nu=\frac{1}{3}$.

It has been previously[1] pointed out that the short wavelength limit of the lower branch is physically meaningless because, as the wavelength approaches the shell thickness, neglect of the bending energy is certainly not justified. For spherical shells, Kalnins[6] has shown that the upper branch of the spectrum represents true membrane modes in which the strain energy is primarily extensional, while the inclusion of bending stiffness increases the frequencies of the lower branch modes significantly for large values of n. It is reasonable to assume that the same qualitative behavior is exhibited by a spheroidal shell.

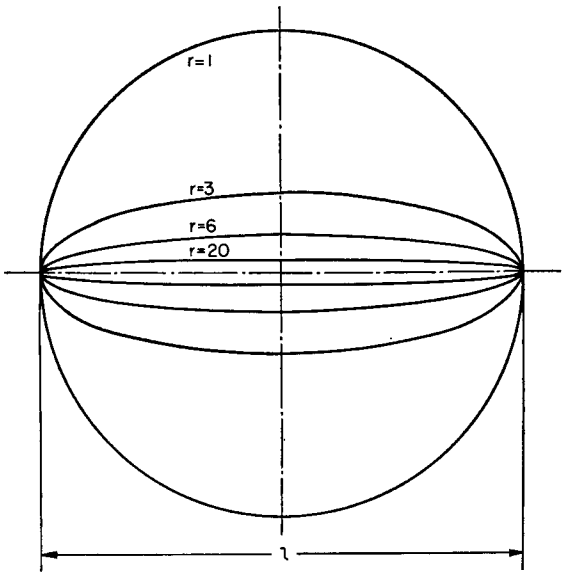

FIG. 6. Geometry of middle surfaces of shells of constant length l and varying ratios $r=l/R$ of length of equatorial radius.

TABLE I. Comparison of Computed frequency and mode shape with previously obtained values for $r=\sqrt{2}$, $\nu=\frac{1}{3}$, $n=2$.

	MODE SHAPE WITH U(0.05)=1		COMMENT
λ	$U(0.7)$	$W(0.7)$	
3.31	9.61	5.38	computed by perturbation in Ref. 2
3.39	9.73	5.30	computed by method of this paper, $N=20$
3.53	...	...	computed by Rayleigh–Ritz method in Ref. 1

TABLE II. Comparison of computed frequencies and mode shapes for $a=100$ with exact values for spherical shell, $\nu=\frac{1}{3}$.

	λ FOR n=2	MODE SHAPES FOR n=4 WITH U(0.05)=1	
		$U(0.5)$	$W(0.5)$
exact	1.4170	3.63	10.82
computed, $N=20$	1.4172	3.61	10.79

[6] A. Kalnins, "Effect of Bending on the Vibrations of Spherical Shells," J. Acoust. Soc. Am. 36, 74–81 (1964).

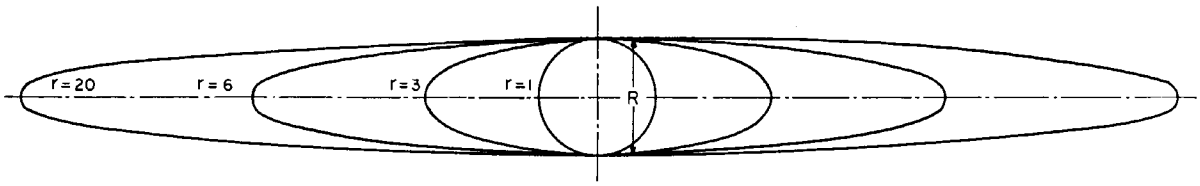

FIG. 7. Geometry of middle surfaces of shells of constant equatorial radius R and varying ratios l/R of length to equatorial radius.

IV. NUMERICAL RESULTS FOR $\nu=\frac{1}{3}$

In Fig. 3, the upper and lower branches of the λ-versus-n mode spectrum are shown for a prolate spheroid with $r=\sqrt{2}$ and for the circular geometry $r=1$. It is seen that the asymptotic limit frequency, corresponding to $\lambda=2(1+\nu)r^2$, is below the lowest frequency of the upper branch. In all mode spectra presented, of course, only ordinates for integral values of n are physically meaningful.

Lower branches of the mode spectrum are plotted in Fig. 4 for comparison of shells of constant length and in Fig. 5 for comparison of shells of constant equatorial radius. It should be reemphasized that the same data are plotted in Figs. 4 and 5. As has been pointed out in Sec. III, both plots are desirable, since X is a measure of relative frequency for shells of constant equatorial radius but differing eccentricities while λ is a similar measure for shells of constant length. It is to be noted that the computed frequencies approach the predicted limiting values of Eqs. 35 very well.

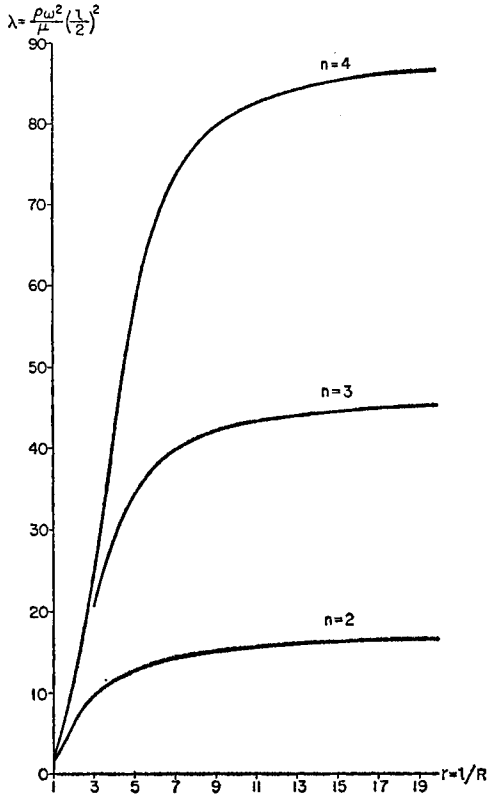

FIG. 8. Plot of frequency parameter λ for shells of constant length l vs ratio r of length to equatorial radius with mode number n as parameter.

Further confirmation of the accuracy of the computed results may be had by (a) comparing calculated values for $r=\sqrt{2}$ with results previously obtained by Silbiger and DiMaggio[1] and by Shiraishi and DiMaggio,[2] respectively, and (b) comparing calculated values for a very large value of a with exact values for the spherical case.[5] Such comparisons are shown in Tables I and II.

Although mode shapes as well as frequencies were obtained simultaneously, mode shapes are not presented herein because their qualitative shape is obvious and extensive tabular listings of values at pivotal points appears inappropriate, especially since programming the numerical algorithm presented is an elementary matter.

It should be pointed out that the transition from the curve from $r=3$ to that for the spherical case $r=1$ in Fig. 5 is continuous but becomes evident only for $r\leq\sqrt{2}$. Thus, a plot of frequency versus eccentricity at a given mode number for shells of equal equatorial radius is not monotonic whereas, as can be seen in Fig. 4; it is monatonic for shells of equal length.

In Figs. 6 and 7, the geometries of the middle surfaces of the shells of constant length and equatorial radius whose mode spectra are plotted in Figs. 4 and 5, respectively, are illustrated.

In Fig. 8, the mode spectrum of Fig. 4 is replotted with mode number instead of eccentricity as parameter. This allows easier interpolation for intermediate frequencies.

ACKNOWLEDGMENTS

This investigation was sponsored by the U. S. Office of Naval Research under contract with Columbia University.

Appendix A. Listing of Significant Functions

$$\theta_1=g(a^2-\eta^2)(g\beta-f_6^2),$$

$$\theta_2=\eta f_6[gf_4+2gf_6-g(a^2-\eta^2)(2\beta-1) -2f_6f_5(a^2-\eta^2)], \tag{A1}$$

$$\theta_3=g^2(a^2-\eta^2)\left[1+\frac{\lambda(a^2-\eta^2)}{2a^2}\right]+gf_4\eta^2(1-\eta^2) -f_6(1-\eta^2)[g(a^2-3\eta^2)+2f_5\eta^2(a^2-\eta^2)];$$

$$\psi_1=\frac{f_6(a^2-\eta^2)(a^2-1)^{\frac{1}{2}}}{ag}, \tag{A2}$$

$$\psi_2=\frac{\eta(a^2-\eta^2)(a^2-1)^{\frac{1}{2}}}{ag},$$

where

$$g=-\frac{\lambda}{2a^4}(a^2-1)(a^2-\eta^2)^3+\beta(a^2-\eta^2)^2 +2(a^2-1)(a^2-\eta^2)(\beta-1)+\beta(a^2-1)^2; \tag{A3}$$

$$f_4=2\beta(a^2-1)+a^2-\eta^2,$$

$$f_5=-\frac{3\lambda}{2a^4}(a^2-1)(a^2-\eta^2)^2 +2\beta(a^2-\eta^2)+2(a^2-1)(\beta-1), \tag{A4}$$

$$f_6=-\beta(a^2-1)-(\beta-1)(a^2-\eta^2),$$

in which

$$\beta=1/(1-\nu). \tag{A5}$$